Supplementary Information
for
Synergistic Solutions: Reverse Osmosis and Nanofiltration Configurations for Efficient Brackish Water Desalination

Submitted: May 20, 2025

Arianna Tariqi[a], Luis Cruzado[b], Anthony P. Straub[c], Kerri L. Hickenbottom[a*], and Vasiliki Karanikola [a *]

[a]*Department of Chemical and Environmental Engineering, University of Arizona, Tucson, AZ 85721, USA*

[b]*Bureau of Reclamation, Yuma Desalting Plant, Yuma, AZ 06520, USA*

[c]*Department of Civil, Environmental, and Architectural Engineering, University of Colorado Boulder, Boulder, CO 80309, USA*

[*] Corresponding Authors:

Vasilki Karanikola: phone: 520-621-5881; e-mail: vkaranik@arizona.edu
Kerri Hickenbottom: phone: 520-626-9323; e-mail: klh15@arizona.edu

A manuscript prepared for publication in:
Nature Partner Journals Clean Water

Number of Pages: 19

Number of Tables: 5

Number of Figures: 11

S1. ***Total dissolved solids concentration and salt rejection for piloted systems***

The total dissolved solids (TDS) concentrations and salt rejection for particular ions for the reverse osmosis (RO) and nanofiltration (NF) configurations, such as RO-RO, RO-NF90, NF90-RO, NF270-p-RO, and RO-c-NF270, are shown in **Table S1** and **Table S2**, respectively. Water samples from the feed, permeate, and concentrate of the first and second stages of the pilot system were analyzed weekly. The permeate TDS measurements from stage 1 and stage 2 were averaged to get the overall permeate TDS concentration for the RO-RO, RO-NF90, and NF90-RO. The ion concentrations for calcium, magnesium, sodium, potassium, chloride, and sulfate for the permeate and feed streams were analyzed to find salt rejections for the first and second stage of each configuration. The overall permeate TDS concentration for NF270-p-RO configuration is only from stage 2, and the overall permeate for RO-c-NF270 is from the first stage (See **Fig. S3-S7**). The RO-RO had the lowest first stage and overall TDS concentrations. The NF90-RO configuration had the highest overall TDS concentration. The hybrid NF270-p-RO and RO-RO conventional systems had similar permeate TDS concentrations.

Table S1. *TDS concentrations from the feed and permeate of the first and second stages of the piloted hybrid nanofiltration and reverse osmosis configurations.*

Configuration	Feed water TDS mg/L	1st stage permeate TDS mg/L	2nd stage feed TDS mg/L	2nd stage permeate TDS mg/L	Overall permeate TDS mg/L
RO-RO	1991	9	4261	16	10
RO-NF90	1987	10	4031	142	29
NF90-RO	2012	92	4250	34	40
NF270-p-RO	1912	1424	1424	11	11
RO-c-NF270	2076	20	4895	2881	20

Table S2. *Ion rejections for chloride, sodium, potassium, magnesium, calcium, and sulfate of the first and second stages of the piloted hybrid nanofiltration and reverse osmosis configurations*

Configurations	Stage	Chloride	Sodium	Potassium	Magnesium	Calcium	Sulfate
RO-RO	1st stage	99.44%	99.66%	99.29%	100.00%	99.99%	99.61%
	2nd stage	99.48%	99.54%	99.38%	99.98%	100.00%	99.71%
RO-NF90	1st stage	99.43%	99.61%	99.78%	100.00%	99.90%	99.60%
	2nd stage	95.89%	96.68%	96.41%	99.77%	99.77%	99.46%
NF90-RO	1st stage	96.48%	97.08%	96.88%	99.66%	99.66%	99.38%
	2nd stage	98.95%	99.08%	99.02%	99.98%	99.98%	99.72%
NF270-p-RO	1st stage	21.30%	52.98%	53.43%	86.18%	85.50%	96.60%
	2nd stage	99.27%	98.99%	98.56%	99.93%	98.16%	88.68%
RO-c-NF270	1st stage	99.04%	99.22%	98.67%	99.97%	98.80%	99.34%
	2nd stage	2.90%	35.95%	31.60%	72.31%	71.44%	91.46%

S2. *Model and experimental data verification*

The RO-RO baseline experimental data were used to verify the modeled parameters' outputs. The model was simulated on Water Application Value Engine (WAVE) design software (version 1.82, DuPont Water and Process Solutions, 2023). The feed water quality measurements of the Yuma Desalting Plant, temperature, flows, and water recovery are based on the experimental data. The experimental system required a flow bypass between the first and second stages, therefore the model was set to the corrected recovery of the system (bypass flow was subtracted from the feed flow). A bypass between stages cannot be modeled on WAVE; therefore, a pre-stage pressure difference was added to the first stage because of the experimental differential pressure between the pump discharge and the pressure vessel inlet (~200 kPa difference). Additionally, a pre-stage pressure difference of 100 kPa was added to the second stage of the model to account for the pressure losses due to the bypassed flow. After the two-stage system was modeled, the second stage was modeled separately to acquire the driving pressure associated with the feed flow and recovery. For the NF90-RO and NF270-p-RO configurations, the booster pump pressure was calculated based on the required feed of the second stage or pass. The trends in the pressure of the first and second stage are similar between the model and experimental data. Any variability between the model and experimental data is likely a result of the assumptions, design constraints, and operational fluctuations.

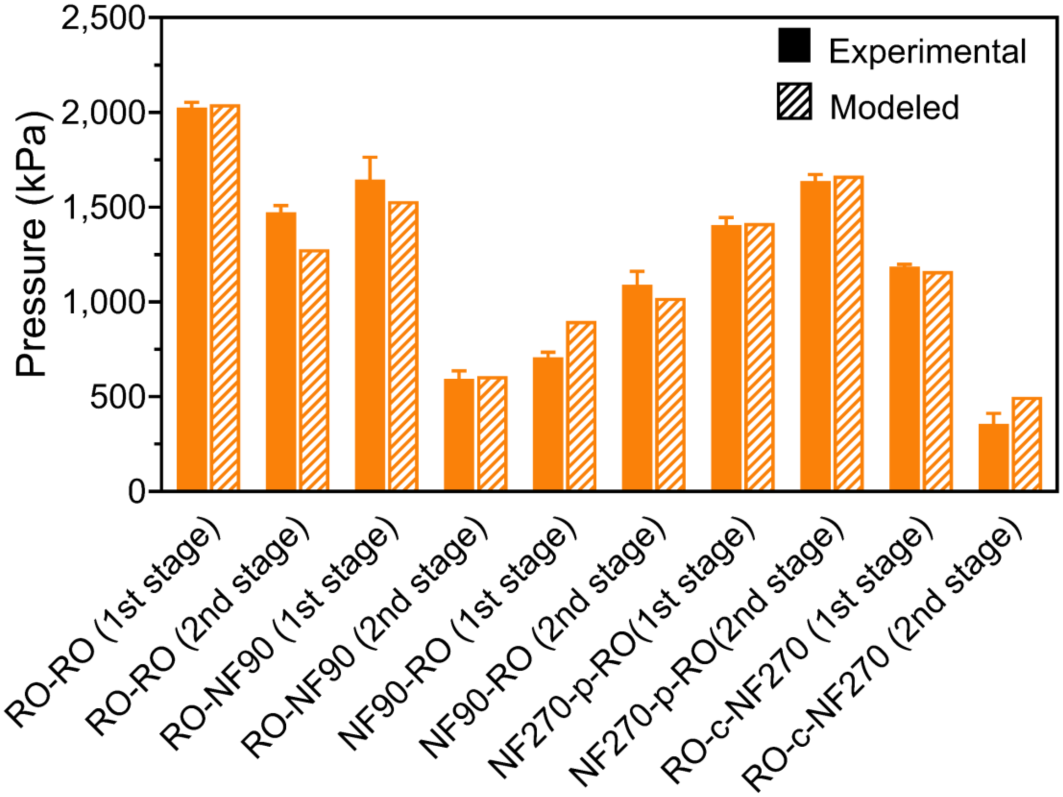

Fig. S1. Pressure values of the modeled and experimental results of the RO-RO baseline, RO-NF90, NF90-RO, NF270-p-RO, and RO-c-NF270 configurations per stage. The experimental pressures are displayed as a solid orange bar, and the modeled pressures are shown as an orange diagonal striped bar. The water recovery, feed flow, and feed characteristics are based on the pilot system results. The second stage and pass were modeled separately to correct for the bypass flow in between the first and second stage. To consider the pressure changes, a 100 kPa pre-stage pressure difference was added to the second stages of the model, and temperature was specified to experimental conditions. ranging from 22 – 30°C depending on the configuration. The error bars are the standard deviation of the experimental data.

S3. *Saturation Indices of modeled configurations*

Table S3. *Modeled saturation indices of the RO-RO, RO-NF90, NF90-RO, NF270-p-RO, and RO-c-NF270 configurations of the RO concentrate.*

Configuration	$CaSO_4$ saturation (%)	$BaSO_4$ saturation (%)	$SrSO_4$ saturation (%)	SiO_2 saturation (%)
RO-RO	54.8	617.5	31.1	30
RO-NF90	55.2	613.8	30.9	29.4
NF90-RO	55.3	613.3	30.9	29.3
NF270-p-RO	8.3	87	4.4	84.1
RO-c-NF270	46.7	513.3	25.6	52.3

S4. ***Fractional Contribution of modeled configurations***

The RO-RO, RO-NF90, NF90-RO, RO-NF90, NF270-p-RO, and RO-c-NF270 were modeled on the Water Application Value Engine (WAVE) design software (version 1.82, DuPont Water and Process Solutions, 2023). The model was designed to produce 1 million gallons per day (MGD) of water and a base recovery of 72%. The pressures and designs of each system varied depending on the goal of each configuration.

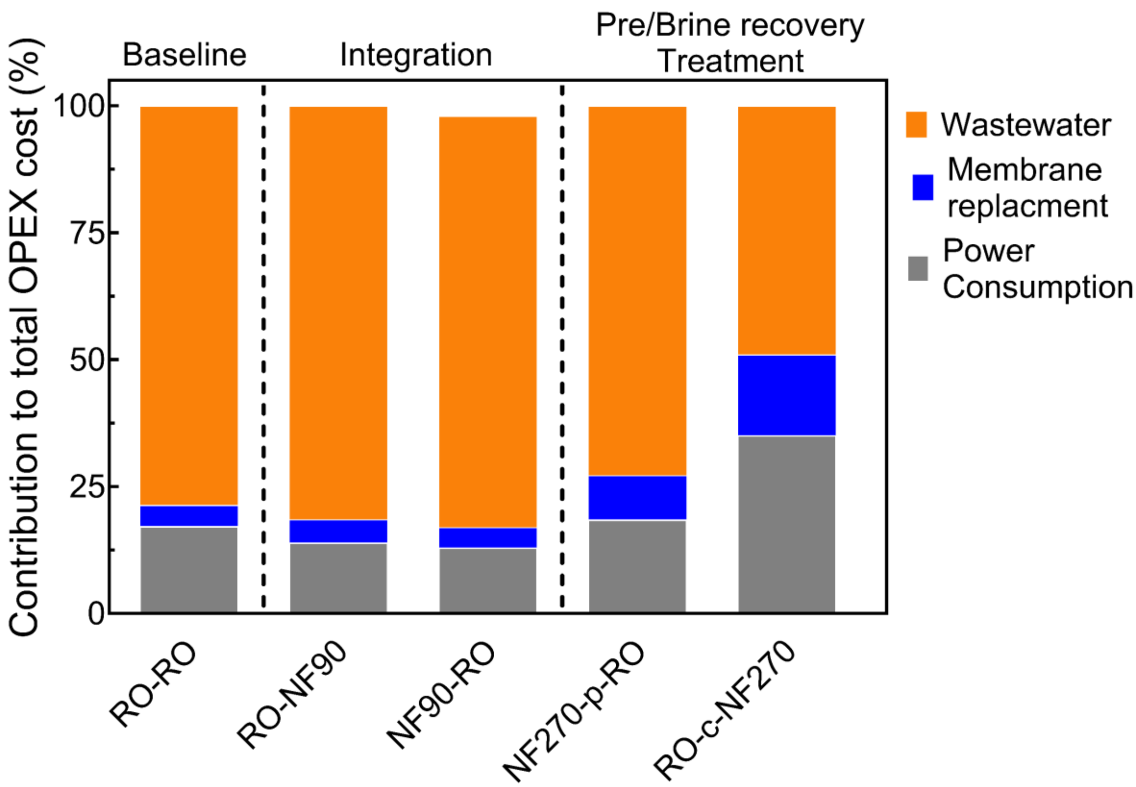

Fig. S2. Fractional contribution cost of the operational expenditures (OPEX) for a baseline RO-RO system and four hybrid configurations. The orange color represents the cost associated with wastewater disposal, the blue color represents the cost of membrane replacement, and the gray color represents the cost of power consumption. Wastewater has less influence on the RO-c-NF270 configurations than the other systems because of the permeate recycle stream in the second stage (NF270). Overall, wastewater has the highest contribution to the overall variable operating costs of the systems. Other costs, such as chemical and capital costs, were considered the same for each system and, therefore, not included in the analysis.

S5. ***Element screening unit pilot system schematic and general equations***

The RO-RO, RO-NF90, NF90-RO, NF270-p-RO, and RO-c-NF270 configurations were piloted at the Yuma Desalting Plant (YDP) on the Element Screening Unit (ESU). The configurations each represent a hybrid configuration utilizing NF and RO membranes in either the first or second stage. The first stage of the ESU had two pressure vessels in series whereas the second stage had one pressure vessel, each with two membranes each. The system was situated in a 2:1 array. The general equations of the technical performance of the system are shown in Table S2.

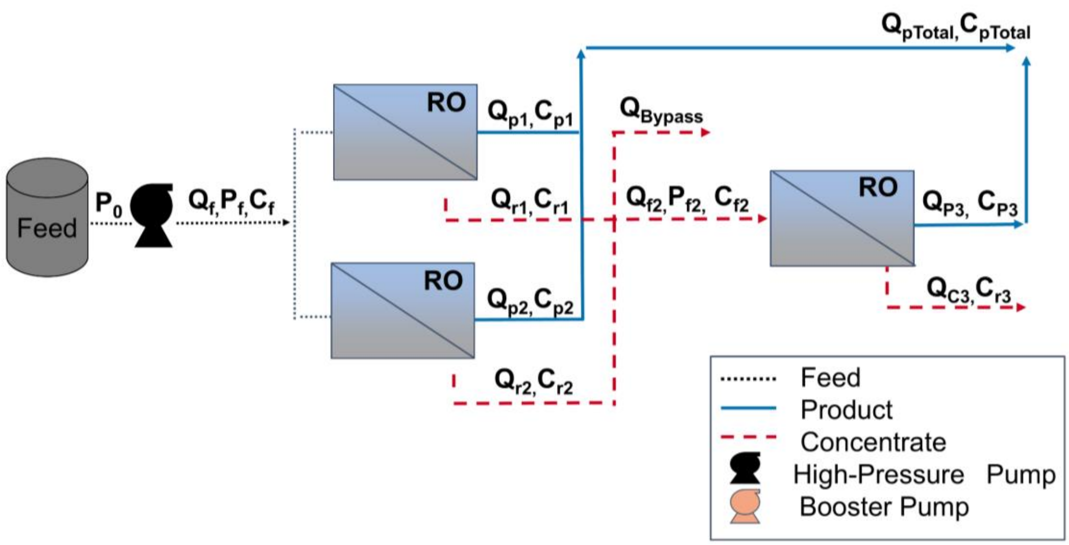

Fig. S3. Schematic of the RO-RO configuration resembling conventional reverse osmosis configurations. The first and second stages contained RO membranes (BW30). The concentrate flow of the first stage was the feed flow to the second stage. The bypass valve directed a portion of water flow from the first stage concentrate water to the drain. The first and second stage permeate flow is the total product water from the system. The concentrate flow from the second stage is the total brine flow.

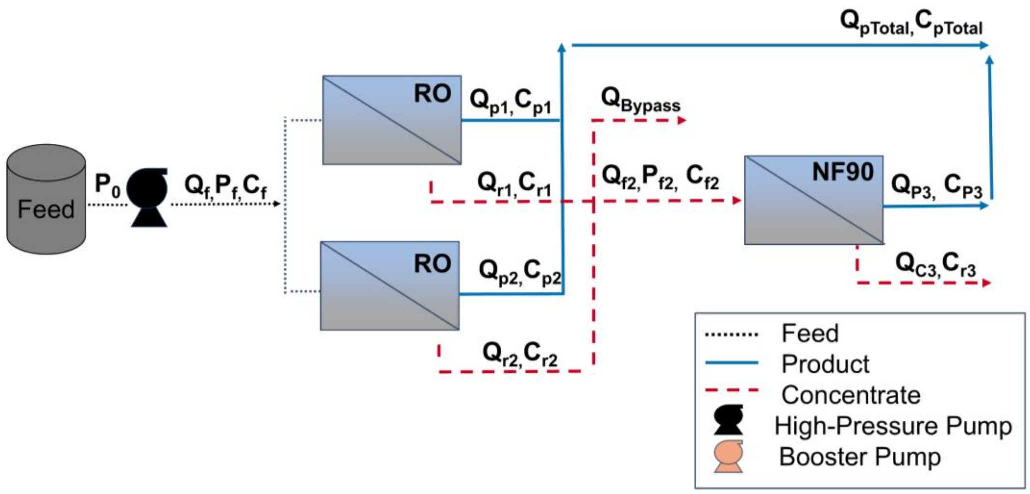

Fig. S4. Schematic of the RO-NF90 configuration. The NF90 membranes are used in the second stage instead of RO membranes. The concentrate flow of the first stage is the feed flow of the second stage. The bypass valve directs a portion of the first stage concentrate flow to the drain. The first and second stage permeate flow is the total product water from the system. The concentrate flow from the second stage is the total brine flow.

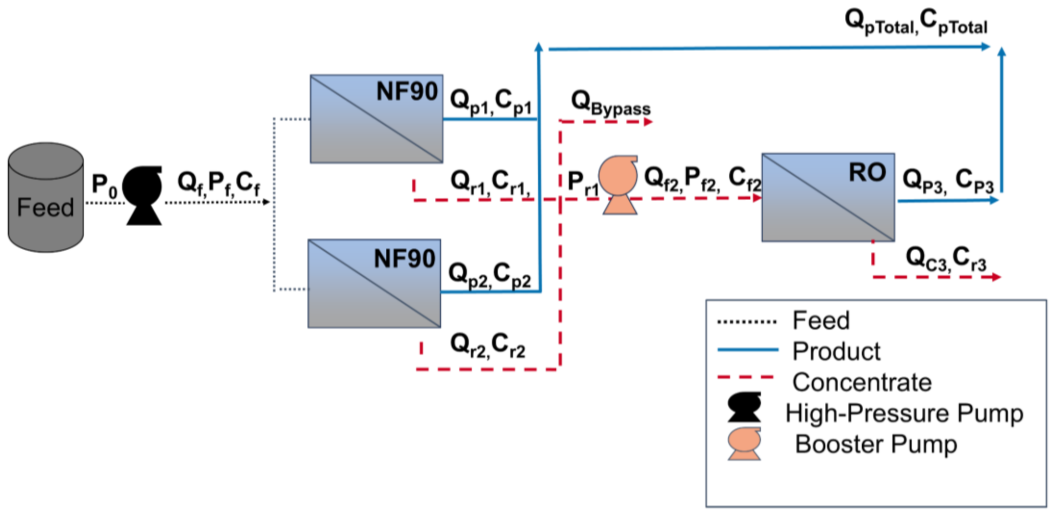

Fig. S5. Schematic of the NF90-RO configuration. The NF90 membranes are used in the first stage instead of RO membranes. The concentrate flow of the first stage is the feed flow of the second stage. The bypass valve directs a portion of the first stage concentrate flow to the drain. The first and second stage permeate flow is the total product water from the system. The concentrate flow from the second stage is the total brine flow.

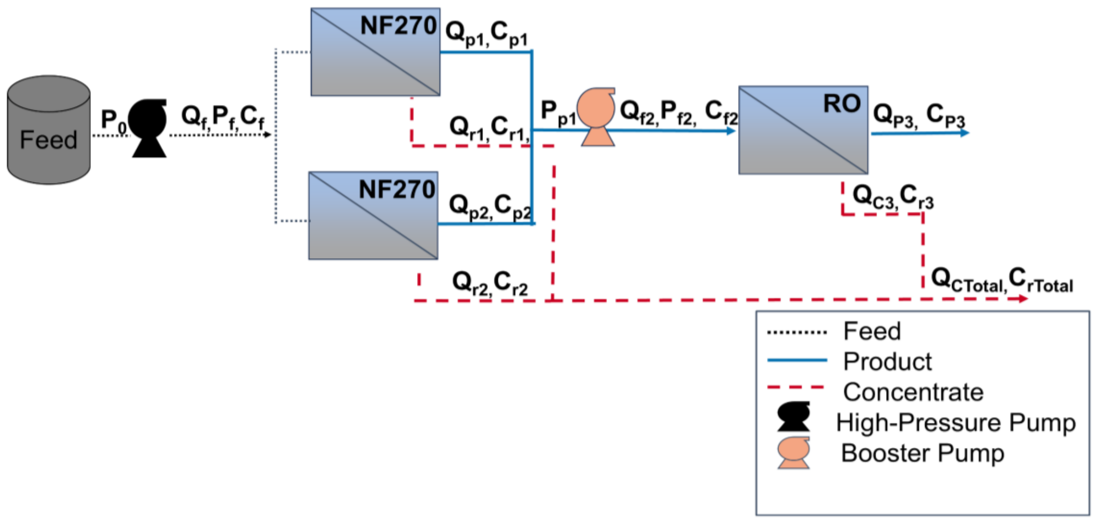

Fig. S6. Schematic of the NF270-p-RO configuration. The NF270 membranes are used in the first stage to pretreat the feed water before entering the RO membranes in the second stage. The permeate flow of the first stage is the feed flow of the second stage. A booster pump is required in between the first and second stages since the pressure requirements of RO are higher than an NF270. The second stage permeate flow is the total product water from the system. The concentrate flow from the first and second stage is the total brine flow.

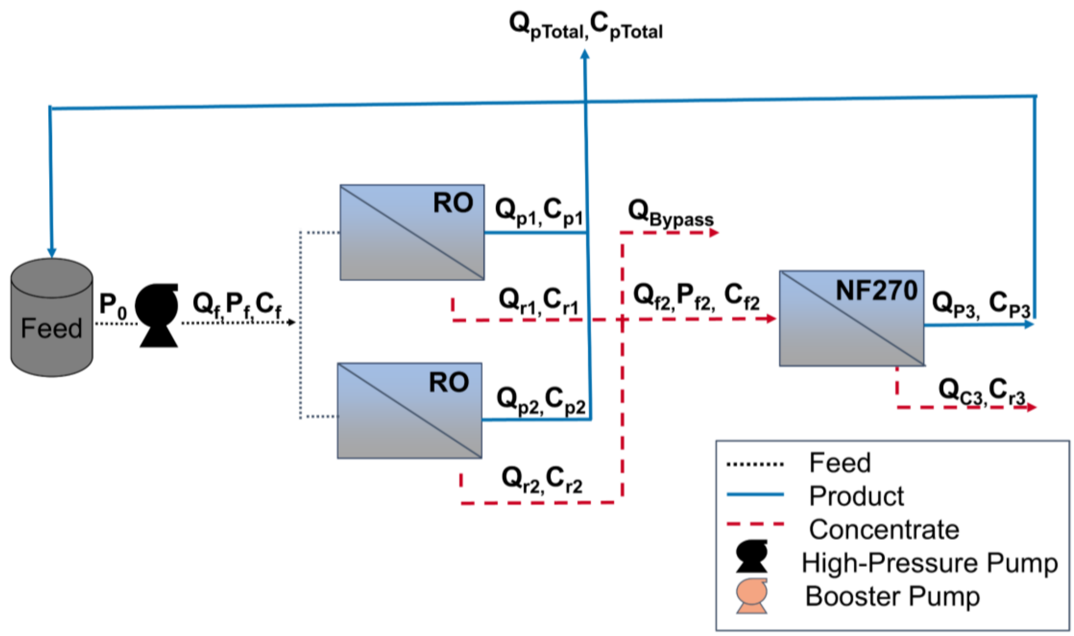

Fig. S7. Schematic of the RO-c-NF270 configuration. The NF270 are used in the second stage to recover brine of the RO concentrate and send the remaining permeate to the feed tank before entering the RO membranes. The system requires a bypass valve to direct a portion of the concentrate water from the first stage to the drain. The total permeate flow was from the first stage only. The concentrate flow from the first and second stages are the total brine flow.

Fig. S8. Image of the element screening unit at the Yuma Desalting Plant. Pictures are the three pressure vessels with two membranes each. The top two pressure vessel are the first stage in series. The last pressure vessel is the second stage. The high pressure pump (not pictured) is used to feed the brackish water from the feed tank to the first stage pressure vessels.

Table S4. *Detailed mathematical equations for the pilot RO-RO, RO-NF90, NF90-RO, NF270-p-RO, and RO-c-NF270 configurations.*

	Description	Unit	Equation
General pilot equations [a]	1st stage recovery	%	$\frac{Q_{p1}+Q_{p2}}{Q_{f1}} \times 100$
	2nd stage recovery	%	$Q_{p3}/Q_{f2} \times 100$
	Corrected recovery	%	$\frac{(Q_{p1}+Q_{p2}+Q_{p3}-Q_{Bypass})}{Q_{f1}} \times 100$
	Intrinsic recovery	%	$\frac{Q_{p1}+Q_{p2}+Q_{p3}}{Q_{f1}} \times 100$
	1st stage salt rejection	%	$\left(1-\frac{C_{p1}+C_{p2}}{C_{f1}}\right) \times 100$
	2nd stage salt rejection	%	$\left(1-\ C_{p3}/C_{f2}\right) \times 100$
	Overall salt rejection	%	$\left(1-\frac{Avg\ (C_{p1,}\ C_{p2,}\ C_{p3}\ )}{C_{f1}}\right) \times 100$
	1st stage water flux	LMH	$\left(\frac{Q_{p2}+Q_{p1}}{4*A_m}\right)$
	2nd stage water flux	LMH	$\left(Q_{p3}/2*A_m\right)$
	1st stage salt flux	$\frac{kg}{m^2hr}$	$(J_{w1})*(Avg\ C_{p1}\&\ C_{p2})$
	2nd stage salt flux	$\frac{kg}{m^2hr}$	$(J_{w2})*(Avg\ C_{p3})$
Specific pilot equations	Corrected recovery of NF270-p-RO	%	$Q_{p3}/Q_{f1} \times 100$
	Overall salt rejection of NF270-p-RO	%	$\left(1-\ C_{p3}/C_{f1}\right) \times 100$
	Overall recovery of RO-c-NF270	%	$\frac{(Q_{p1}+Q_{p2}-Q_{Bypass})}{Q_{f1}-Q_{p3}} \times 100$

	Corrected recovery of RO-c-NF270	%	$$\frac{(Q_{p1}+Q_{p2})}{Q_{f1}-Q_{p3}}\times 100$$
[a] Pilot and model equations are general to the RO-RO, RO-NF90, NF90-RO, NF270-p-RO, and RO-c-NF270 unless stated otherwise to specific systems			

S6. ***Modeled system schematics and general equations***

The RO-RO, RO-NF90, NF90-RO, RO-NF90, NF270-p-RO, and RO-c-NF270 were modeled on the WAVE design software (version 1.82, DuPont Water and Process Solutions, 2023). The model was designed to produce 1 MGD of water and a base recovery of 72%. The pressures and designs of each system varied depending on the goal of each configuration.

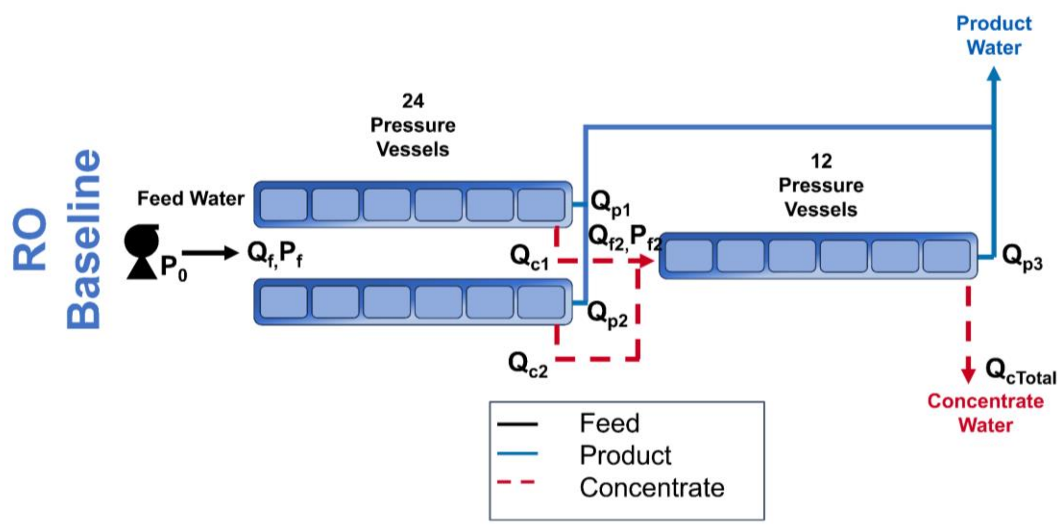

Fig. S9. Schematic of the modeled RO-RO, RO-NF90, and NF90-RO. The recovery of the systems is set to 72% with a feed flow of 1.4 MGD. The first and second stages have 24 and 12 pressure vessels in series, respectively, making a 2:1 ratio design. The pressure vessels have six membranes in each. The total permeate flow is a combination of the first and second stage permeate flow. The total concentrate flow is from the second stage. The feed pressure differs between configurations. The NF90-RO configuration required a booster pump between the first stage (NF90) and second stage (RO), therefore each stage was modeled separately.

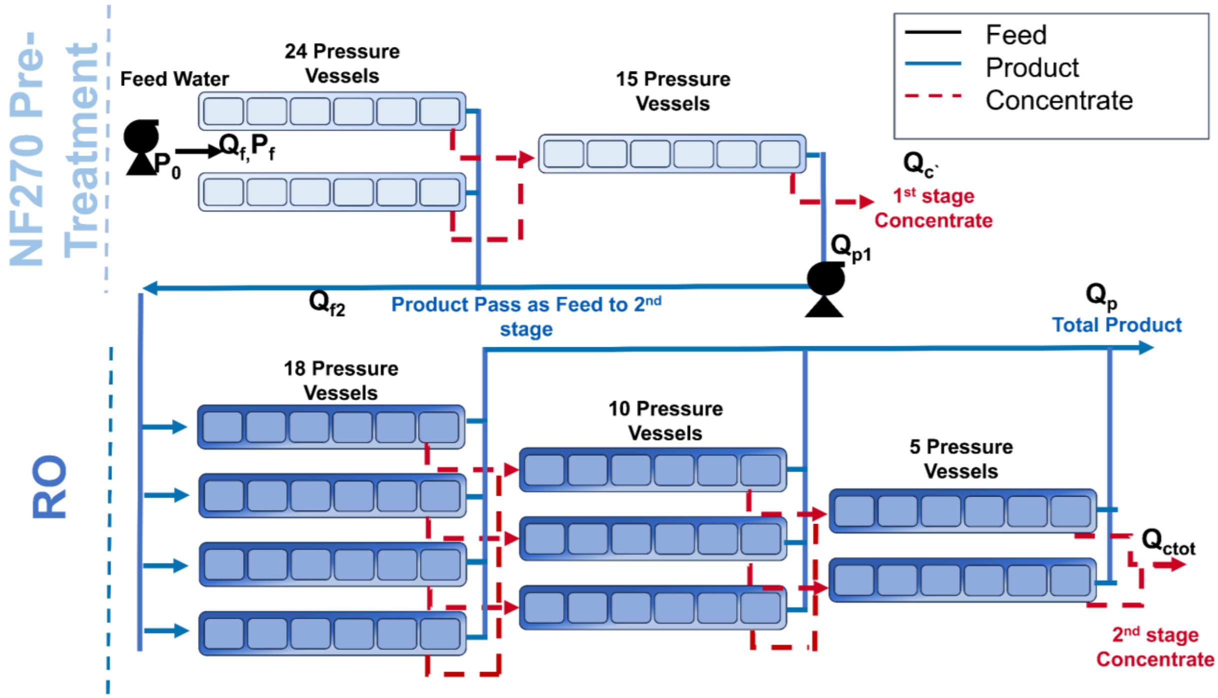

Fig. S10. Schematic of the modeled NF270-p-RO. The water recovery is 72% and the feed flow is 1.4 MGD. The system is a two-pass design. The first pass is similar to the RO-RO configuration with 24 and 15 pressure vessels in the first and second stages, respectively, making a 2:1 ratio design. The second pass consists of three stages with 18, 10, and 5 pressure vessels in the first, second, and third stage, respectively. The pressure vessels have seven elements in the each pressure vessel of the first pass and six elements in the second pass. The three stages are in a 4:2:1 ratio to maximize recovery. The second stage permeate flow is the total permeate flow (1 MGD). The total concentrate flow is from the first and second pass.

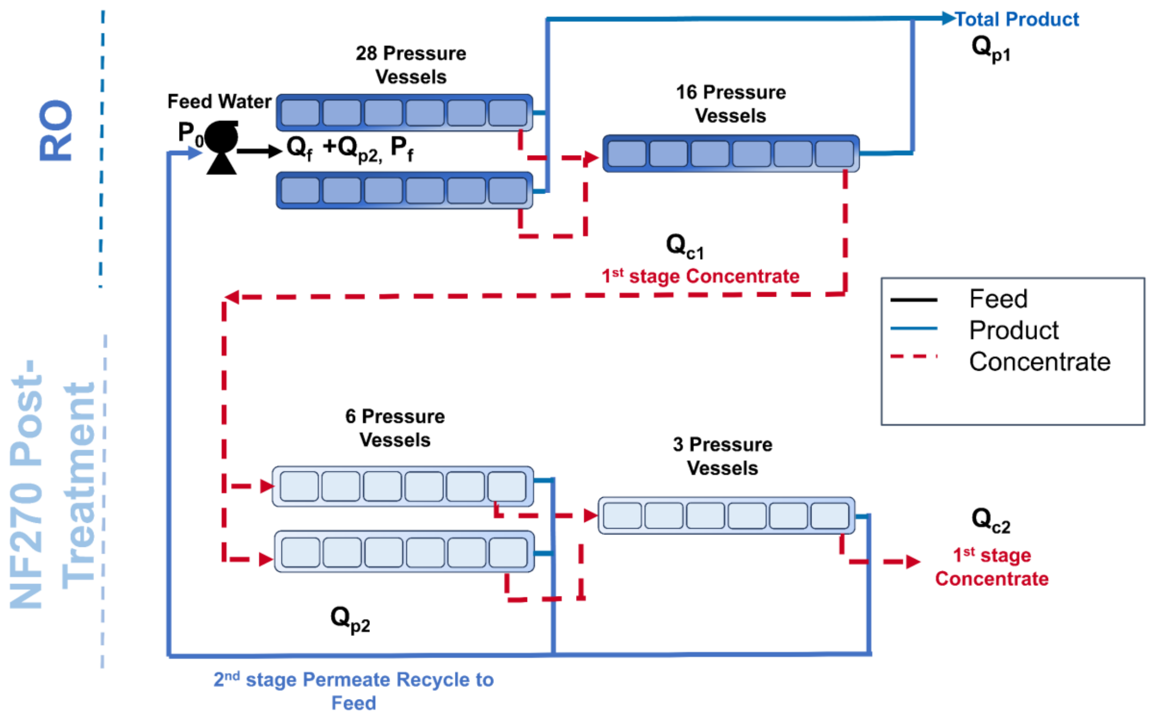

Fig. S11. Schematic of the RO-c-NF270. The water recovery is 72% with an additional 71% recovery from the recycle stream of the post-treatment stages (stages 3 and 4). The feed flow was 1.4 MGD. Stages 1 and 2 resemble the RO-RO configuration with a 2:1 ratio design. The pressure vessels have seven membranes in each. The post-treatment stages consisted of 6 and 3 pressure vessels in the first and second, respectively, making a 2:1 ratio design. The permeate flow of the NF270 stages are recycled to the feed of the RO stages. The total concentrate flow is the total flow from the all four stages.

Table S5. *Detailed mathematical equations for the modeled RO-RO, RO-NF90, NF90-RO, NF270-p-RO, and RO-c-NF270 configurations*

	Description	Unit	Equation
General equations for model [a]	Specific energy consumption	$\frac{kwh}{m^3}$	$\frac{\left((P_f - P_0) \times Q_f\right)}{(Q_{p1}+Q_{p2}+Q_{p3}) \times \eta_{HP}}$
	Overall cost of high pressure pump	$\frac{\$}{yr}$	$\frac{(P_f \times Q_f \times D_{EP})}{\eta_{HP}}$
	Overall cost of wastewater	$\frac{\$}{yr}$	$(WWcost \times Q_{CTotal})$
	Operation expenses (OPEX)	$\frac{\$}{m^3}$	$\frac{(OC_{HP} + OC_{WW} + OC_{memR})}{365 \times (Q_{p1+}Q_{p2+}Q_{p3})}$
System specific equations	Specific energy consumption of RO-NF90	$\frac{kwh}{m^3}$	$\frac{\left((P_f - P_0) \times Q_f\right) + \left((P_{f2} - P_c) \times Q_{f2}\right.}{(Q_{p1}+Q_{p2}+Q_{p3}) \times \eta_{BP} \times \eta_{HP}}$
	OPEX of RO-NF90 and NF270-p-RO	$\frac{\$}{m^3}$	$\frac{(OC_{HP} + OC_{BP} + OC_{WW} + OC_{memR})}{365 \times (Q_{pTot})}$
	Specific energy consumption of NF270-p-RO	$\frac{kwh}{m^3}$	$\frac{\left((P_f - P_0) \times Q_f\right) + \left((P_{f2} - P_p) \times Q_{f2}\right.}{Q_{pTot} \times \eta_{BP} \times \eta_{HP}}$
	Overall cost of booster pump of NF90-RO and NF270-p-RO	$\frac{\$}{yr}$	$\frac{((P_{f2} - P_{f,out}) \times (Q_{f2} - Q_{p1}) \times D_{EP})}{\eta_{BP}}$
	Specific energy of RO-c-NF270	$\frac{kwh}{m^3}$	$\frac{\left((P_f - P_0) \times \left((Q_f)\right)\right)}{(Q_{pTot}) \times \eta_{HP}}$
	Overall cost of wastewater	$\frac{\$}{yr}$	$(WWcost \times (Q_{c1} + Q_{c2}))$

[a] Pilot and model equations are general to the RO-RO, RO-NF90, NF90-RO, NF270-p-RO, and RO-c-NF270 unless stated otherwise to specific systems